

## Structure–Activity Studies of 14-Helical Antimicrobial $\beta$ -Peptides: Probing the Relationship between Conformational Stability and Antimicrobial Potency

Tami L. Raguse,<sup>†</sup> Emilie A. Porter,<sup>†</sup> Bernard Weisblum,<sup>‡</sup> and Samuel H. Gellman<sup>\*,†</sup>

Contribution from the Department of Chemistry and Department of Pharmacology,  
University of Wisconsin, Madison, Wisconsin 53706

Received May 24, 2002

**Abstract:** Antimicrobial  $\alpha$ -helical  $\alpha$ -peptides are part of the host-defense mechanism of multicellular organisms and could find therapeutic use against bacteria that are resistant to conventional antibiotics. Recent work from Hamuro et al. has shown that oligomers of  $\beta$ -amino acids (" $\beta$ -peptides") that can adopt an amphiphilic helix defined by 14-membered ring hydrogen bonds (" $\beta$ -14-helix") are active against *Escherichia coli* [Hamuro, Y.; Schneider, J. P.; DeGrado, W. F. *J. Am. Chem. Soc.* **1999**, *121*, 12200–12201]. We have created two series of cationic 9- and 10-residue amphiphilic  $\beta$ -peptides to probe the effect of 14-helix stability on antimicrobial and hemolytic activity. 14-Helix stability within these series is modulated by varying the proportions of rigid *trans*-2-aminocyclohexanecarboxylic acid (ACHC) residues and flexible acyclic residues. We have previously shown that a high proportion of ACHC residues in short  $\beta$ -peptides encourages 14-helical structure in aqueous solution [Appella, D. H.; Barchi, J. J.; Durell, S. R.; Gellman, S. H. *J. Am. Chem. Soc.* **1999**, *121*, 2309–2310]. Circular dichroism of the  $\beta$ -peptides described here reveals a broad range of 14-helix population in aqueous buffer, but this variation in helical propensity does not lead to significant changes in antibiotic activity against a set of four bacteria. Several of the 9-mers display antibiotic activity comparable to that of a synthetic magainin derivative. Among these 9-mers, hemolytic activity increases slightly with increasing 14-helical propensity, but all of the 9-mers are less hemolytic than the magainin derivative. Previous studies with conventional peptides ( $\alpha$ -amino acid residues) have provided conflicting evidence on the relationship between helical propensity and antimicrobial activity. This uncertainty has arisen because  $\alpha$ -helix stability can be varied to only a limited extent among linear  $\alpha$ -peptides without modifying parameters important for antimicrobial activity (e.g., net charge or hydrophobicity); a much greater range of helical stability is accessible with  $\beta$ -peptides. For example, it is very rare for a linear  $\alpha$ -peptide to display significant  $\alpha$ -helix formation in aqueous solution and manifest antibacterial activity, while the linear  $\beta$ -peptides described here range from fully unfolded to very highly folded in aqueous solution. This study shows that  $\beta$ -peptides can be unique tools for analyzing relationships between conformational stability and biological activity.

### Introduction

Multicellular organisms employ diverse, short peptides to defend against microbial invaders.<sup>1–3</sup> Host-defense peptides are usually cationic, and they appear to act by permeabilizing microbial membranes, although other mechanisms of action have been proposed. Many of these peptides display specific secondary structures in the presence of target membranes.  $\alpha$ -Helical conformations are adopted, for example, by magainins<sup>4,5</sup> (from frogs) and cecropins<sup>6</sup> (from insects). The folded forms tend to

be highly amphiphilic, with cationic side chains and hydrophobic side chains segregated into distinct regions of the molecular surface. The amphiphilicity is presumably related to the mode of action: cationic charge directs the peptides to anionic bacterial membranes, and hydrophobic side chains then interact with the core of the lipid bilayer, ultimately compromising the barrier function of the membrane. Enantiomers of natural host-defense peptides often exert native biological effects,<sup>7,8</sup> implying that antimicrobial activity does not involve interaction between these peptides and specific bacterial protein targets.

Host-defense peptides have been of interest from a therapeutic perspective because their proposed mode of action is not conducive to rapid development of bacterial resistance.<sup>9</sup> These

\* To whom correspondence should be addressed. E-mail: gellman@chem.wisc.edu.

<sup>†</sup> Department of Chemistry.

<sup>‡</sup> Department of Pharmacology.

- (1) Boman, H. G. *Annu. Rev. Immunol.* **1995**, *13*, 61–92.
- (2) Nicolas, P.; Mor, A. *Annu. Rev. Microbiol.* **1995**, *49*, 277–304.
- (3) Hancock, R. E. W.; Chapple, D. S. *Antimicrob. Agents Chemother.* **1999**, *43*, 1317–1323.
- (4) Zasloff, M. *Proc. Natl. Acad. Sci. U.S.A.* **1987**, *84*, 5449–5453.
- (5) Williams, R. W.; Starman, R.; Taylor, K. M. P.; Gable, K.; Beeler, T.; Zasloff, M.; Covell, D. *Biochemistry* **1990**, *29*, 4490–4496.

- (6) Steiner, H.; Hultmark, D.; Engstrom, A.; Bennich, H.; Boman, H. G. *Nature* **1981**, *292*, 246–248.
- (7) Wade, D.; Boman, A.; Wahlin, B.; Drain, C. M.; Andreu, D.; Boman, H. G.; Merrifield, R. B. *Proc. Natl. Acad. Sci. U.S.A.* **1990**, *87*, 4761–4765.
- (8) Bessalle, R.; Kapitkovsky, A.; Gorea, A.; Shalit, I.; Fridkin, M. *FEBS Lett.* **1990**, *274*, 151–155.
- (9) Hancock, R. E. W. *Lancet* **1997**, *349*, 418–422.

peptides or synthetic analogues may provide new tools in the struggle against pathogenic strains that are resistant to conventional antibiotics. This prospect has inspired many structure–activity studies based on natural and designed antimicrobial peptides. Tossi et al.<sup>10</sup> have comprehensively reviewed  $\alpha$ -helical antimicrobial peptides. These authors note that the parameters influencing antimicrobial activity include size, conformational stability, net charge, net hydrophobicity, amphiphilicity, and the widths of the hydrophobic and hydrophilic helix faces. Extraction of general principles from these structure–activity studies can be challenging, however, because sequence alterations frequently affect more than one physical parameter.

Amphiphilic helix-forming oligomers of  $\beta$ -amino acids (“ $\beta$ -peptides”) that display varying degrees of antimicrobial activity have been recently reported.<sup>11–16</sup> Earlier work showed that  $\beta$ -peptides can adopt several distinct helical conformations, depending upon residue substitution pattern.<sup>17–20</sup>  $\beta$ -Peptides comprised of  $\beta$ -substituted residues<sup>21</sup> or  $\alpha$ -substituted residues<sup>22</sup> adopt a “14-helix,” which contains 14-membered ring  $i \rightarrow i-2$  C=O $\cdots$ H–N hydrogen bonds. (The familiar  $\alpha$ -helix of conventional peptides contains 13-membered ring  $i \rightarrow i+4$  C=O $\cdots$ H–N hydrogen bonds.) The 14-helix is observed also when  $\beta$ -peptide residues have a cyclohexyl backbone constraint (e.g., *trans*-2-aminocyclohexanecarboxylic acid (ACHC)).<sup>23,24</sup>  $\beta$ -Peptides with an alternating sequence of  $\alpha$ - and  $\beta$ -substituted residues display a “12/10/12-helix,” which contains both 12-membered ring  $i \rightarrow i+3$  C=O $\cdots$ H–N hydrogen bonds and 10-membered ring  $i \rightarrow i-1$  C=O $\cdots$ H–N hydrogen bonds.<sup>25,26</sup> Use of  $\beta$ -amino acids with a cyclopentyl constraint, for example, *trans*-2-aminocyclopentanecarboxylic acid (ACPC), leads to formation of the “12-helix,” which contains exclusively 12-membered ring  $i \rightarrow i+3$  C=O $\cdots$ H–N hydrogen bonds.<sup>27,28</sup> Oligomers of  $\beta$ -amino acids constrained by *cis*-substituted oxetane rings adopt a “10-helical” conformation, which contains 10-membered ring  $i \rightarrow i-1$  C=O $\cdots$ H–N hydrogen bonds.<sup>29</sup>

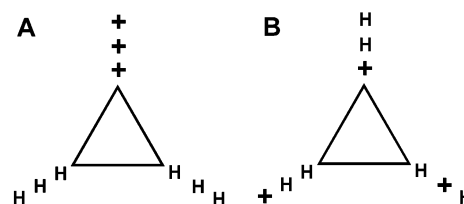


**Figure 1.** Schematic representation of the position of the  $\beta$ -amino acid side chains looking down the 14-helical axis (three residues per turn). Amphiphilic  $\beta$ -peptides **1–7** are represented by illustration A and non-amphiphilic **8** is represented by B. Positively charged  $\beta^3$ -homolysine side chains are designated by + and hydrophobic side chains of ACHC,  $\beta^3$ -homoleucine, and  $\beta^3$ -homovaline are designated by H.  $\beta^3$ -Homotyrosine side chains of **5–8** are not shown.

Antimicrobial activity has been observed for both 14-helical<sup>11,13</sup> and 12-helical<sup>12,14,16</sup>  $\beta$ -peptides. The 14-helix has approximately three residues per turn; DeGrado and co-workers<sup>11,13</sup> prepared antimicrobial versions by linking hydrophobic-cationic-hydrophobic residue triads to one another (as shown in Figure 1A). The resulting 14-helices have a polar surface that comprises roughly one-third (120°) of the helix circumference.<sup>11,13</sup> The 12-helix, on the other hand, has approximately 2.5 residues per turn. Antimicrobial versions were generated by linking cationic-hydrophobic-cationic-hydrophobic-pentads (one pentad = two helical turns), to give 12-helices with a polar surface that covers roughly two-fifths (ca. 144°) of the helix circumference.<sup>12,14,16</sup>

Here, we examine structure–activity relationships among 14-helical  $\beta$ -peptides. We are particularly interested in the relationship between conformational stability and biological activity.  $\beta$ -Peptides are intriguing subjects from this perspective since the 14-helical propensity of an individual residue can be profoundly enhanced by switching from an acyclic backbone to a cyclohexane-constrained backbone. We have reported a homologous series of hexa- $\beta$ -peptides in which the proportion of cyclohexane-constrained and acyclic ( $\beta$ -substituted) residues was varied.<sup>30</sup> High population of the 14-helix was observed in aqueous solution when four or more of the six residues were cyclohexane-constrained, but little or no 14-helix could be detected in the absence of cyclohexane-constrained residues. The  $\alpha$ -helical stability of conventional peptides cannot be modulated to this large extent because no  $\alpha$ -amino acid residues have sufficient folding propensity to generate  $\alpha$ -helices at the hexamer length.

Several groups have evaluated the relationship between  $\alpha$ -helical stability and biological activity for antimicrobial peptides, but the results have varied from system to system.<sup>10</sup> In almost every case it has been necessary to compare extents of  $\alpha$ -helix formation within a series in trifluoroethanol (TFE)/water mixtures because the peptides do not fold detectably in water; the antimicrobial studies, of course, have been conducted in aqueous solution. Some groups have examined the effect of enhancing  $\alpha$ -helical stability. Chen et al.<sup>31</sup> showed that changing two glycines in magainin II to alanine led to enhanced  $\alpha$ -helicity in aqueous TFE and to greater antibiotic activity against several

- (10) Tossi, A.; Sandri, L.; Giangaspero, A. *Biopolymers* **2000**, *55*, 4–30.  
 (11) Hamuro, Y.; Schneider, J. P.; DeGrado, W. F. *J. Am. Chem. Soc.* **1999**, *121*, 12200–12201.  
 (12) Porter, E. A.; Wang, X. F.; Lee, H. S.; Weisblum, B.; Gellman, S. H. *Nature* **2000**, *404*, 565.  
 (13) Liu, D.; DeGrado, W. F. *J. Am. Chem. Soc.* **2001**, *123*, 7553–7559.  
 (14) Porter, E. A.; Weisblum, B.; Gellman, S. H. *J. Am. Chem. Soc.* **2002**, *124*, 7324–7330.  
 (15) Arvidsson, P. I.; Frackenhof, J.; Ryder, N. S.; Liechty, B.; Petersen, F.; Zimmermann, H.; Camenisch, G. P.; Woessner, R.; Seebach, D. *ChemBioChem* **2001**, *2*, 771–773.  
 (16) LePlae, P. R.; Fisk, J. D.; Porter, E. A.; Weisblum, B.; Gellman, S. H. *J. Am. Chem. Soc.* **2002**, *124*, 6820–6821.  
 (17) Seebach, D.; Matthews, J. L. *Chem. Commun.* **1997**, 2015–2022.  
 (18) Gellman, S. H. *Acc. Chem. Res.* **1998**, *31*, 173–180.  
 (19) DeGrado, W. F.; Schneider, J. P.; Hamuro, Y. *J. Pept. Res.* **1999**, *54*, 206–217.  
 (20) Gademann, K.; Hintermann, T.; Schreiber, J. V. *Curr. Med. Chem.* **1999**, *6*, 905–925.  
 (21) Seebach, D.; Overhand, M.; Kühnle, F. N. M.; Martinoni, B.; Oberer, L.; Hommel, U.; Widmer, H. *Helv. Chim. Acta* **1996**, *79*, 913–941.  
 (22) Hintermann, T.; Seebach, D. *Synlett* **1997**, 437–438.  
 (23) Appella, D. H.; Christianson, L. A.; Karle, I. L.; Powell, D. R.; Gellman, S. H. *J. Am. Chem. Soc.* **1999**, *121*, 6206–6212.  
 (24) Appella, D. H.; Christianson, L. A.; Karle, I. L.; Powell, D. R.; Gellman, S. H. *J. Am. Chem. Soc.* **1996**, *118*, 13071–13072.  
 (25) Seebach, D.; Abele, S.; Gademann, K.; Guichard, G.; Hintermann, T.; Jaun, B.; Matthews, J. L.; Schreiber, J. V.; Oberer, L.; Hommel, U.; Widmer, H. *Helv. Chim. Acta* **1998**, *81*, 932–982.  
 (26) Seebach, D.; Gademann, K.; Schreiber, J. V.; Matthews, J. L.; Hintermann, T.; Jaun, B.; Oberer, L.; Hommel, U.; Widmer, H. *Helv. Chim. Acta* **1997**, *80*, 2033–2038.  
 (27) Appella, D. H.; Christianson, L. A.; Klein, D. A.; Powell, D. R.; Huang, X. L.; Barchi, J. J.; Gellman, S. H. *Nature* **1997**, *387*, 381–384.  
 (28) Applegate, J.; Bode, K. A.; Appella, D. H.; Christianson, L. A.; Gellman, S. H. *J. Am. Chem. Soc.* **1998**, *120*, 4891–4892.

- (29) Claridge, T. D. W.; Goodman, J. M.; Moreno, A.; Angus, D.; Barker, S. F.; Taillefer, C.; Watterson, M. P.; Fleet, G. W. *J. Tetrahedron Lett.* **2001**, *42*, 4251–4255.  
 (30) Appella, D. H.; Barchi, J. J.; Durell, S. R.; Gellman, S. H. *J. Am. Chem. Soc.* **1999**, *121*, 2309–2310.  
 (31) Chen, H. C.; Brown, J. H.; Morell, J. L.; Huang, C. M. *FEBS Lett.* **1988**, *236*, 462–466.

bacterial species. In contrast, Houston et al.<sup>32</sup> found that stabilizing the  $\alpha$ -helical conformation of cecropin-melittin hybrids by introducing lactam bridges between glutamic acid and lysine side chains (*i, i+4*) led to a decrease in antimicrobial activity, relative to noncyclized analogues. The cyclized peptides displayed partial  $\alpha$ -helix formation in aqueous solution, while the noncyclized analogues displayed substantial  $\alpha$ -helix formation only in aqueous TFE. These authors concluded that excessive  $\alpha$ -helix stability is detrimental to antimicrobial activity.

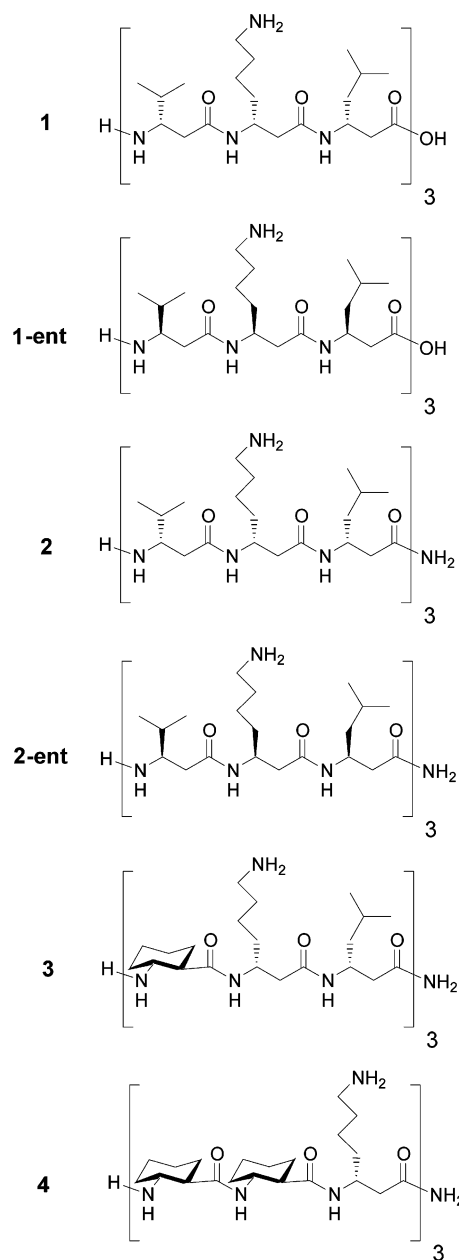
Complementary studies have involved  $\alpha$ -helix destabilization, either by incorporation of D residues or by incorporation of proline. Dathe et al.<sup>33</sup> reported a systematic study based on a designed 18-residue peptide containing only lysine, leucine, and alanine that forms an amphiphilic  $\alpha$ -helix. These workers compared the all-L peptide to nine diastereomers in which adjacent residue pairs had D configuration. The double-D replacements diminished  $\alpha$ -helical stability, with the greatest effect from replacements at the center of the sequence. Interestingly, the least stable diastereomer displayed only a 3-fold decrease in  $\alpha$ -helix population relative to the all-L isomer in aqueous TFE. Double-D replacements at the termini had relatively little effect on antimicrobial activity (*Escherichia coli* and *Staphylococcus epidermidis*), but replacements at the center caused significant diminution of activity, up to a 16-fold increase in minimal inhibitory concentration (MIC). Chen et al.<sup>31</sup> found that introducing three D-alanine residues into a magainin analogue increased MIC values by 10- to 100-fold relative to the all-L diastereomer. In contrast, Shai and Oren found that incorporating several D residues into the toxins pardaxin<sup>34</sup> or melittin<sup>35</sup> had little effect on antimicrobial activity. Zhang et al.<sup>36</sup> compared several related peptides containing zero, one, or two prolines. In general, antimicrobial activity decreased as the number of prolines increased (variations in this trend may have resulted from other sequence changes). These workers summarized conflicting results obtained by others regarding the effect of proline introduction or removal on antimicrobial activity. Overall, the available results from conventional peptide studies do not provide consistent conclusions regarding the relationship between  $\alpha$ -helical stability and antimicrobial activity.

Peptides that disrupt bacterial membranes cannot have therapeutic utility unless they leave human cell membranes intact. Human cell membrane susceptibility to physical disruption is generally evaluated via hemolysis (lysis of red blood cells). In most of the studies cited above,  $\alpha$ -helix destabilization led to a decrease in hemolytic activity. In some cases, the diminution of hemolytic activity was greater than the effect on antibacterial activity, leading some workers to propose that  $\alpha$ -helical stability is more important for the former than the latter.<sup>33–35</sup> Indeed, Shai and co-workers have reported amphiphilic peptides with features designed to minimize  $\alpha$ -helicity (e.g., 33% D residues; N-to-C cyclization) that show significant antimicrobial activity but little hemolytic activity.<sup>37</sup>

Here we compare nine- and ten-residue  $\beta$ -peptides that form flexible amphiphilic 14-helices with analogues that have been rigidified by incorporation of the cyclohexyl-rigidified ACHC residue. The residues replaced by ACHC,  $\beta^3$ -homovaline and  $\beta^3$ -homoleucine, are expected to have hydrophobicities comparable to that of ACHC. The  $\beta$ -peptides containing ACHC display at least partial 14-helix in aqueous solution, while the  $\beta$ -peptides containing only acyclic residues do not; therefore, these  $\beta$ -peptides allow us to examine the effect of very high helical propensity on biological activity without resorting to side chain bridging, a modification that is required for  $\alpha$ -helix stabilization among conventional peptides.<sup>38</sup>

## Results

**Design.** We based the sequences of  $\beta$ -peptides **1–4** on **1-ent**, reported by Hamuro et al.<sup>11</sup> to have moderate activity against *E. coli*. We expected that increasing the proportion of ACHC residues from zero ( $\beta$ -peptide **2**) to two-thirds ( $\beta$ -peptide **4**)



(32) Houston, M. E.; Kondejewski, L. H.; Karunaratne, D. N.; Gough, M.; Fidai, S.; Hodges, R. S.; Hancock, R. E. W. *J. Pept. Res.* **1998**, *52*, 81–88.

(33) Dathe, M.; Schumann, M.; Wieprecht, T.; Winkler, A.; Beyermann, M.; Krause, E.; Matsuzaki, K.; Murase, O.; Bienert, M. *Biochemistry* **1996**, *35*, 12612–12622.

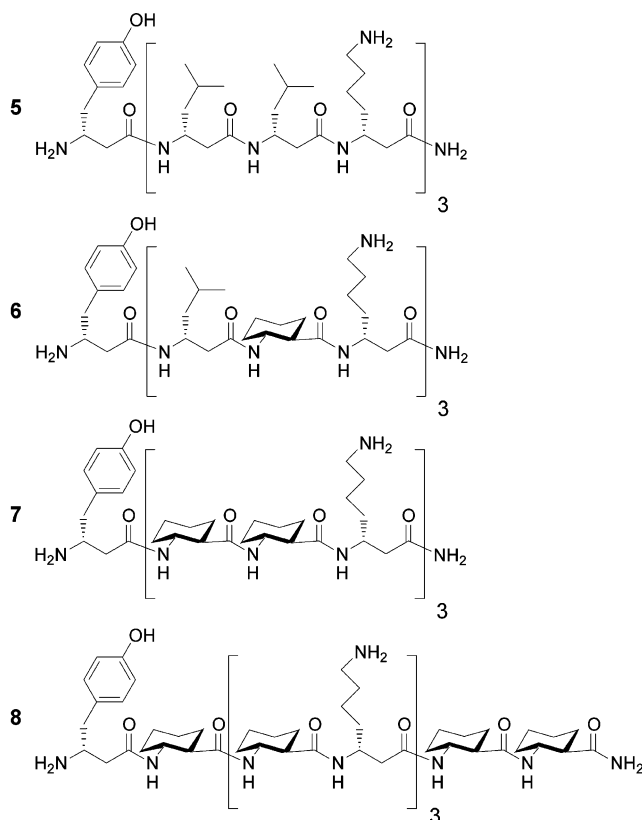
(34) Shai, Y.; Oren, Z. *J. Biol. Chem.* **1996**, *271*, 7305–7308.

(35) Oren, Z.; Shai, Y. *Biochemistry* **1997**, *36*, 1826–1835.

(36) Zhang, L.; Benz, R.; Hancock, R. E. W. *Biochemistry* **1999**, *38*, 8102–8111.

(37) Oren, Z.; Shai, Y. *Biochemistry* **2000**, *39*, 6103–6114.

would also increase the amount of 14-helical structure in aqueous solution. The  $\beta$ -peptide 14-helix has approximately three residues per turn, giving rise to a helical triad repeat in which every third residue is on the same face of the helix.  $\beta$ -Peptide **4** contains a cationic-hydrophobic-hydrophobic triad repeat in place of the hydrophobic-cationic-hydrophobic triad repeat found in **1–3** because we originally believed that coupling ACHC to the resin would be difficult.<sup>39</sup> We have recently evaluated the ability of  $\beta$ -peptides **5–8** to form small



soluble aggregates in aqueous solution as an initial step toward the creation of  $\beta$ -peptide tertiary structure.<sup>40</sup> Since **5–7** were designed to form amphiphilic 14-helices, we evaluated  $\beta$ -peptides **5–7** and **8**, a nonamphiphilic isomer of **7**, for antimicrobial activity as well. Most  $\beta$ -peptides we prepared were of opposite absolute stereochemistry relative to **1-ent**, since (*R,R*)-ACHC is more synthetically accessible than its enantiomer.<sup>41</sup> All  $\beta$ -peptides except **8** were designed to be amphiphilic when adopting the 14-helical conformation, with hydrophobic residues covering roughly two-thirds of the helix circumference and mostly positively charged  $\beta^3$ -homolysine residues on the remaining third of the helix circumference (Figure 1).

We replaced the C-terminal carboxylic acid group of **1** with a carboxamide in  $\beta$ -peptide **2** because analogous C-terminal capping enhances antimicrobial activity among conventional peptides.<sup>35,42,43</sup> Since the C-terminal amide gave much higher

antimicrobial activity, this feature was retained in all subsequent  $\beta$ -peptides. We compared **2** and **2-ent** to determine whether the absolute stereochemistry of  $\beta$ -peptides affects their biological activity.

We used circular dichroism (CD) data obtained in aqueous solution to compare the intrinsic 14-helix stabilities among our  $\beta$ -peptides. For two sets of homologous  $\beta$ -peptides with incrementally increasing backbone rigidification, **2–4** and **5–7**, 14-helix stability was compared with both antimicrobial and hemolytic activity. The importance of helical amphiphilicity on these biological activities was determined by comparing two highly rigidified  $\beta$ -peptide isomers, **7**, which will form an amphiphilic 14-helix, and **8**, which will form a nonamphiphilic 14-helix (Figure 1). The  $\alpha$ -helical  $\alpha$ -peptides melittin and (Ala<sup>8,13,18</sup>)-magainin II amide (a synthetic derivative of natural magainin II with enhanced antimicrobial activity<sup>31</sup>) were used as controls in determinations of biological activity. Both (Ala<sup>8,13,18</sup>)-magainin II amide and melittin are active against a broad spectrum of bacteria, but melittin is toxic toward both bacterial and mammalian cells,<sup>6,44,45</sup> while (Ala<sup>8,13,18</sup>)-magainin II amide is selectively toxic toward bacterial cells.<sup>4</sup>

**Synthesis of  $\beta$ -Peptides.**  $\beta$ -Peptides **1–8**, **1-ent**, and **2-ent** were synthesized from Fmoc-protected  $\beta$ -amino acid monomers<sup>46,47</sup> using standard automated solid-phase Fmoc chemistry. However, during the synthesis of  $\beta$ -peptide **3**, the Fmoc protecting group was not completely removed from the 6th and 7th residues with the standard deprotection conditions, 20% piperidine in DMF. Reversed-phase high-performance liquid chromatography (RP-HPLC) and matrix-assisted laser desorption–ionization time-of-flight mass spectral (MALDI-TOF-MS) analysis of the crude product showed that the Fmoc-protected hexamer and heptamer were present along with the desired nonamer.<sup>48</sup> During the synthesis of an analogous  $\beta$ -peptide, we encountered a similar problem: neither the use of the stronger base DBU nor longer deprotection times with 20% piperidine in DMF led to complete removal of the Fmoc protecting group from the 5th residue of the  $\beta$ -peptide attached to the resin. However, when the same peptide-resin was deprotected at 60 °C in 20% piperidine in NMP, the Fmoc protecting group was completely removed. Therefore, deprotections were performed at 60 °C after the 6th and 7th residues during the synthesis of **3**. The problematic deprotections of the 5th and 6th residues of **6** were also performed at 60 °C.

**Circular Dichroism.** Several recent studies show that CD data can provide insight on  $\beta$ -peptide folding,<sup>49</sup> analogously to the way CD illuminates secondary structure formation in  $\alpha$ -peptides.<sup>50,51</sup> The right-handed 14-helical conformation of  $\beta$ -peptides is characterized by a maximum in molar ellipticity

(38) Houston, M. E.; Gannon, C. L.; Kay, C. M.; Hodges, R. S. *J. Pept. Sci.* **1995**, *1*, 274–282.

(39) Preliminary results in our laboratory had shown that coupling of ACHC to the resin proceeded in low yield. However, we observed no incomplete coupling of ACHC to the resin during the subsequent synthesis of **8**.

(40) Raguse, T. L.; Lai, J. R.; LePlae, P. R.; Gellman, S. H. *Org. Lett.* **2001**, *3*, 3963–3966.

(41) Appella, D. H.; LePlae, P. R.; Raguse, T. L.; Gellman, S. H. *J. Org. Chem.* **2000**, *65*, 4766–4769.

(42) Cuervo, J. H.; Rodriguez, B.; Houghten, R. A. *Pept. Res.* **1988**, *1*, 81–86.

(43) Li, Z. Q.; Merrifield, R. B.; Boman, I. A.; Boman, H. G. *FEBS Lett.* **1988**, *231*, 299–302.

(44) Blondelle, S. E.; Houghten, R. A. *Biochemistry* **1991**, *30*, 4671–4678.

(45) Habermann, E. *Science* **1972**, *177*, 314–322.

(46) Guichard, G.; Abele, S.; Seebach, D. *Helv. Chim. Acta* **1998**, *81*, 187–206.

(47) Abele, S.; Guichard, G.; Seebach, D. *Helv. Chim. Acta* **1998**, *81*, 2141–2156.

(48) Seebach et al. reported that low purity of some crude  $\beta$ -peptides synthesized on solid support resulted from incomplete removal of the Fmoc protecting group.<sup>47</sup> The use of DBU and longer deprotection times during the synthesis of  $\beta$ -peptides composed entirely of acyclic residues produced favorable results (Seebach, D.; Schreiber, J. V.; Arvidsson, P. I.; Frackenpohl, J. *Helv. Chim. Acta* **2001**, *84*, 271–279).

(49) Cheng, R. P.; Gellman, S. H.; DeGrado, W. F. *Chem. Rev.* **2001**, *101*, 3219–3232.

(50) Johnson, W. C. *Proteins* **1990**, *7*, 205–214.

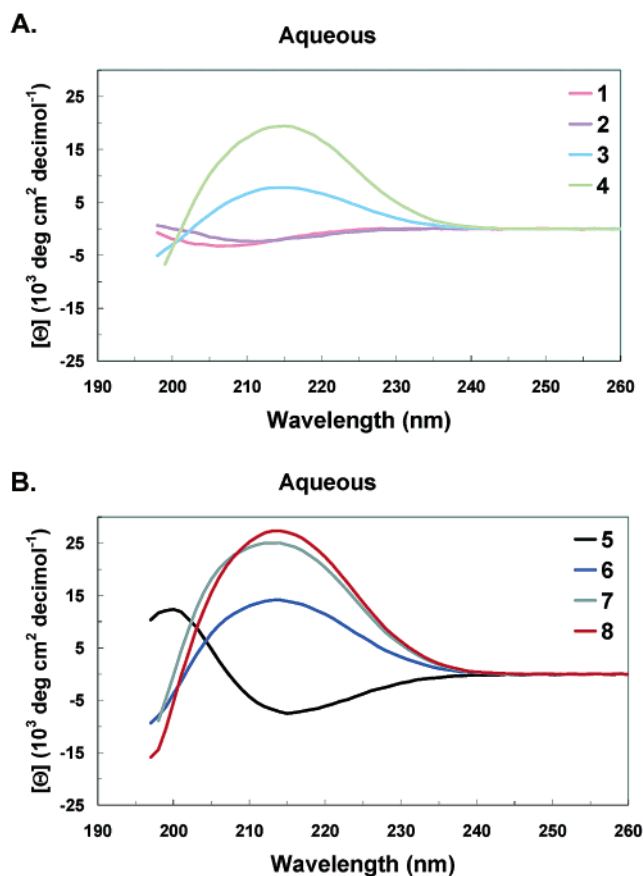


**Figure 2.** Circular dichroism data for  $\beta$ -peptides **1–8** at 25 °C in 10 mM aqueous TRIS, 150 mM NaCl, pH 7.2. Concentrations of  $\beta$ -peptides were approximately 200  $\mu\text{g/mL}$  (approximately 100  $\mu\text{M}$ ).

at approximately 215 nm, and 14-helical  $\beta$ -peptides often display a minimum near 200 nm as well.<sup>52</sup> All of the conformational conclusions we deduce for our  $\beta$ -peptides are based on CD data obtained in aqueous solution. In contrast, as noted above, CD-based conformational analysis of  $\alpha$ -helix-forming antimicrobial  $\alpha$ -peptides is typically carried out in water-TFE mixtures because the peptides do not fold in aqueous solution. (It has been suggested that water-TFE mixtures somehow mimic the hydrophobic environment of cellular membranes,<sup>32</sup> although the physical basis for this hypothesis is unclear.)

CD data for **1–8** in aqueous buffer are shown in Figure 2; part A shows the effect of incremental backbone rigidification among **2–4** while part B shows the analogous rigidification series **5–7**. The  $\beta$ -peptides with the largest proportion of cyclic residues, roughly two-thirds, have the greatest amount of 14-helical structure by CD (**4**, from the first rigidification series, and isomer pair **7** and **8**); as discussed below, we suspect that these  $\beta$ -peptides approach 100% 14-helix population under these conditions. The  $\beta$ -peptides lacking cyclic residues (**1**, **2**, and **5**) do not exhibit a maximum at 214 nm, which suggests that these molecules form little or no 14-helix in aqueous solution.<sup>53</sup> The  $\beta$ -peptides containing roughly one-third cyclic residues (**3** and **6**) seem to be partially folded into the 14-helix under these conditions. Thus, within each rigidification series, the  $\beta$ -peptides

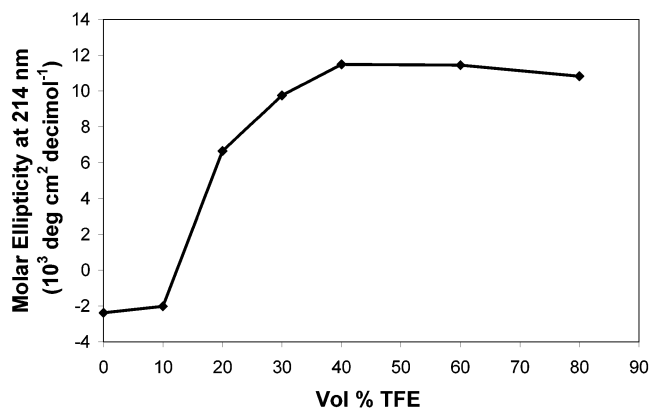


**Figure 3.** Molar ellipticity of 200  $\mu\text{g/mL}$   $\beta$ -peptide **2** in solutions of varying proportions of TFE and aqueous buffer at 25 °C.

range from completely unstructured to largely 14-helical in aqueous solution.

We examined the CD spectra of  $\beta$ -peptides **1–8** in aqueous TFE to gain further insight on the conformational propensities of these molecules. These studies were undertaken because we wanted to know whether the most flexible  $\beta$ -peptides (**1**, **2**, and **5**) would adopt 14-helical conformations, at least to some extent, in the presence of the structure-promoting cosolvent TFE. As noted above,  $\alpha$ -helix induction by TFE is commonly observed for antimicrobial  $\alpha$ -peptides. The CD spectrum of flexible  $\beta$ -peptide **2** was examined at various solvent compositions to discover the TFE/aqueous buffer proportion that produces the maximum amount of 14-helical structure. The data in Figure 3 show that  $\beta$ -peptide **2** displays maximum 14-helicity in  $\geq 40$  vol % TFE in aqueous buffer, as indicated by the molar ellipticity at 214 nm. The plateau in 14-helix induction observed for **1** above 40 vol % TFE matches a similar plateau in  $\alpha$ -helix induction observed for  $\alpha$ -peptides in aqueous TFE.<sup>54</sup> On the basis of these results, we compared the CD spectra of  $\beta$ -peptides **1–8** in 60 vol % TFE (Figure 4), a solvent mixture that we assumed would provide maximal 14-helix induction in each case.

The CD spectra of  $\beta$ -peptides **1–4** and **6–8** in 60 vol % TFE (Figure 4) display maxima in molar ellipticity at 214 nm and exhibit the characteristic signature of the right-handed 14-helix.<sup>55</sup> In contrast,  $\beta$ -peptide **5** does not appear to be 14-helical (Figure 4B). The extent of 14-helix formation in 60 vol % TFE is similar among **1–4** and **6–8**, although there seems to be a slight increase in 14-helicity as the proportion of preorganized AHC residues rises. The most conformationally stable  $\beta$ -peptide, **8**, has only a two-fold greater molar ellipticity at 214 nm relative to flexible  $\beta$ -peptide **2**, which appears to be least structured in 60% TFE. For all three of the  $\beta$ -peptides containing the maximum number of rigid cyclic residues, **4**, **7**, and **8**, the molar ellipticities at 214 nm in aqueous buffer (Figure 2) are equal to or greater than those in 60 vol % TFE (Figure 4). Therefore, we conclude that these three  $\beta$ -peptides are completely folded into the 14-helix, or nearly so, in aqueous buffer.

**Antimicrobial Activity.** Minimal inhibitory concentration (MIC) values for  $\beta$ -peptides **1–8** were determined against both

(51) Yang, J. T.; Wu, C. S.; Martinez, H. M. *Methods Enzymol.* **1986**, *130*, 208–269.

(52) Seebach, D.; Ciceri, P. E.; Overhand, M.; Jaun, B.; Rigo, D.; Oberer, L.; Hommel, U.; Amstutz, R.; Widmer, H. *Helv. Chim. Acta* **1996**, *79*, 2043–2066.

(53) This lack of 14-helical structure in aqueous solution is not surprising. Cheng et al. have concluded that  $\beta^3$ -peptides are less helix-prone than  $\alpha$ -peptides in aqueous solution (Cheng, R. P.; DeGrado, W. F. *J. Am. Chem. Soc.* **2001**, *123*, 5162–5163).

(54) Luo, P.; Baldwin, R. L. *Biochemistry* **1997**, *36*, 8413–8421.

(55)  $\beta$ -Peptide **2-ent**, which is of the opposite absolute configuration, had a minimum molar ellipticity at 214 nm (data not shown).

**Table 1.** MIC Values for Each Peptide in  $\mu\text{g/mL}^a$ 

peptide	<i>E. coli</i> JM109 <sup>b</sup>	<i>B. subtilis</i> BR151 <sup>c</sup>	<i>S. aureus</i> 1206 <sup>d</sup>	<i>E. faecium</i> A634 <sup>e</sup>
(Ala <sup>8,13,18</sup> )-magainin II amide	6.3	3.1	25–50	25
melittin	50	3.1	12.5	6.3
<b>1</b>	200	50	200	$\geq 200$
<b>2</b>	12.5	1.6	6.3	12.5
<b>2-ent</b>	12.5–25	1.6	6.3	12.5–25
<b>3</b>	12.5	0.8	3.1	3.1
<b>4</b>	6.3	0.8	6.3	3.1–6.3
<b>5</b>	12.5	1.6–3.1	6.3	6.3
<b>6</b>	$> 25^f$	0.8	6.3–12.5	3.1–6.3
<b>7</b>	$> 12.5^g$	0.8	12.5	6.3
<b>8</b>	$> 200$	100	$> 200$	$> 200$

<sup>a</sup> Values are the median of at least two independent experiments with two replicates. MICs within a factor of two of each other are considered within experimental uncertainty; therefore, the MICs of two peptides must differ by more than a factor of four for the antimicrobial activity to be considered different beyond experimental uncertainty. <sup>b</sup> Reference 59. <sup>c</sup> Reference 56. <sup>d</sup> Reference 57. <sup>e</sup> Reference 58. <sup>f</sup> Determination of the MIC was not possible because the  $\beta$ -peptide was not soluble above 25  $\mu\text{g/mL}$ . <sup>g</sup> Determination of the MIC was not possible because the  $\beta$ -peptide was not soluble above 12.5  $\mu\text{g/mL}$ .

Gram-positive (*Bacillus subtilis*,<sup>56</sup> *Staphylococcus aureus*,<sup>57</sup> and *Enterococcus faecium*<sup>58</sup>) and Gram-negative (*E. coli*<sup>59</sup>) bacteria. For two of the bacteria, *S. aureus*<sup>57</sup> and *E. faecium*,<sup>58</sup> the strains used are clinical isolates that are resistant to penicillin and vancomycin, respectively (among other antibiotics). The antimicrobial  $\alpha$ -helical  $\alpha$ -peptides melittin<sup>6,44,45</sup> and (Ala<sup>8,13,18</sup>)-magainin II amide<sup>4</sup> served as positive controls.

Most of the  $\beta$ -peptides tested have antimicrobial activity comparable to or more potent than that of the positive controls melittin and (Ala<sup>8,13,18</sup>)-magainin II amide (Table 1); the two exceptions are **1** and **8**. Potency against all four bacterial species increases by one to two orders of magnitude when we replace the C-terminal free carboxylic acid of **1** with a carboxamide in **2**. The antimicrobial activity of **2-ent** is within experimental uncertainty of the activity of its enantiomer, **2**.  $\beta$ -Peptide **8**, which unlike **1–7** cannot form an amphiphilic 14-helix, is inactive against three of the four strains up to the maximum concentration tested.  $\beta$ -Peptide **8** displays weak activity against *B. subtilis*,<sup>56</sup> but amphiphilic isomer **7** is approximately two orders of magnitude more potent against this species. The very feeble activity of **8** relative to **7** indicates that the ability to adopt an amphiphilic structure is very important for antimicrobial action.

$\beta$ -Peptides **2–4** have similar antimicrobial activities despite their vastly different extents of 14-helical structure in aqueous solution (Figure 2A). Likewise,  $\beta$ -peptides **5–7** range from no 14-helical structure to highly structured in aqueous solution (Figure 2B), but the MIC values differ by less than a factor of four among these three  $\beta$ -peptides. Thus, there appears to be little or no relationship between the extent of 14-helix formation in aqueous solution and antimicrobial activity for these two sets of  $\beta$ -peptides.

Minimal bactericidal concentration (MBC) values were determined for selected  $\beta$ -peptides and the control  $\alpha$ -peptide (Ala<sup>8,13,18</sup>)-magainin II amide (Table 2). For each peptide tested, the MBC against *E. coli*<sup>59</sup> and *B. subtilis*<sup>56</sup> was no higher than four times the corresponding MIC. In contrast, most of the MBC values against the resistant strains *S. aureus*<sup>57</sup> and *E. faecium*<sup>58</sup> were greater than the corresponding MIC by at least a factor of eight. Interestingly, with *S. aureus*<sup>57</sup> and *E. faecium*,<sup>58</sup> the

(56) Young, F. E.; Smith, C.; Reilly, B. E. *J. Bacteriol.* **1969**, *98*, 1087–1097.  
 (57) Weisblum, B.; Demohn, V. *J. Bacteriol.* **1969**, *98*, 447–452.  
 (58) Nicas, T. I.; Wu, C. Y.; Hobbs, J. N.; Preston, D. A.; Allen, N. E. *Antimicrob. Agents Chemother.* **1989**, *33*, 1121–1124.  
 (59) Yanisch-Perron, C.; Vieira, J.; Messing, J. *Gene* **1985**, *33*, 103–119.

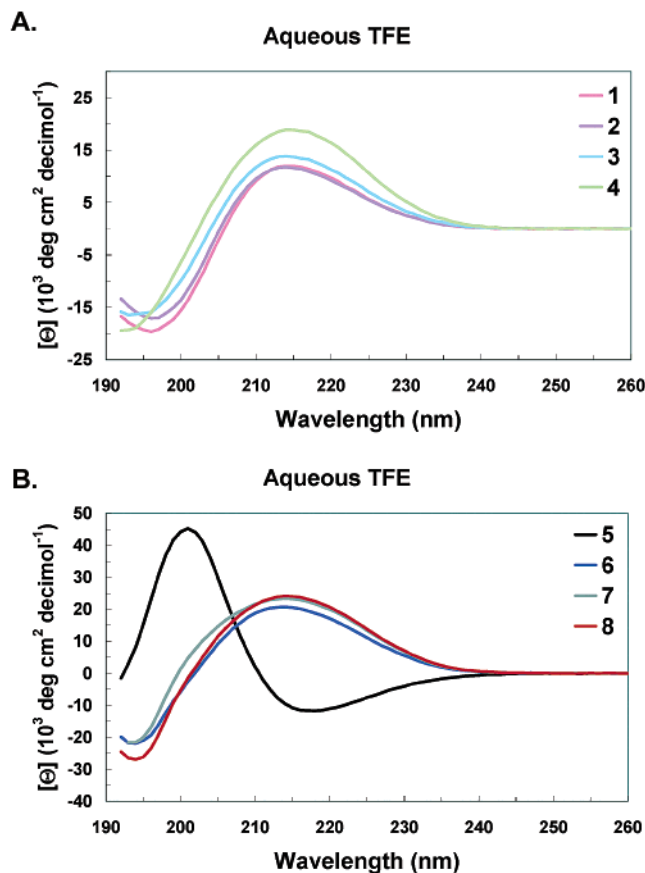


**Figure 4.** Circular dichroism data for  $\beta$ -peptides **1–8** at 25 °C in 60% TFE, 40% TRIS-buffered saline. (Note: The vertical scale in B is different from the scale used in A and in Figure 2.) Concentrations of  $\beta$ -peptides were approximately 200  $\mu\text{g/mL}$  (approximately 100  $\mu\text{M}$ ).

number of viable bacteria after treatment decreased gradually, rather than abruptly, as the concentration of  $\alpha$ - or  $\beta$ -peptide increased. This behavior may be correlated with the fact that these strains of *S. aureus*<sup>57</sup> and *E. faecium*<sup>58</sup> were obtained as clinical isolates. There was very little difference among the MBCs of  $\beta$ -peptides **2–4** for each bacterial species; therefore, bactericidal potency appears to be independent of 14-helical propensity, at least above the minimal propensity displayed by **2**, the most flexible member of this series.

**Hemolytic Activity.** The lysis of human red blood cells (hRBC) by each  $\beta$ -peptide was used to estimate the ability of

**Table 2.** MBC Values for Selected  $\beta$ -Peptides and Control Peptide (Ala<sup>8,13,18</sup>)-Magainin II Amide in  $\mu\text{g/mL}$ 

peptide	<i>E. coli</i> JM109 <sup>a</sup>	<i>B. subtilis</i> BR151 <sup>b</sup>	<i>S. aureus</i> 1206 <sup>c</sup>	<i>E. faecium</i> A634 <sup>d</sup>
(Ala <sup>8,13,18</sup> )-magainin II amide	6.3–12.5	6.3–12.5	>200	>200
2	12.5–25	6.3	$\geq$ 25	>100
3	12.5–25	1.6–3.1	50	>25
4	6.3	1.6	50	>100

<sup>a</sup> Reference 59. <sup>b</sup> Reference 56. <sup>c</sup> Reference 57. <sup>d</sup> Reference 58.

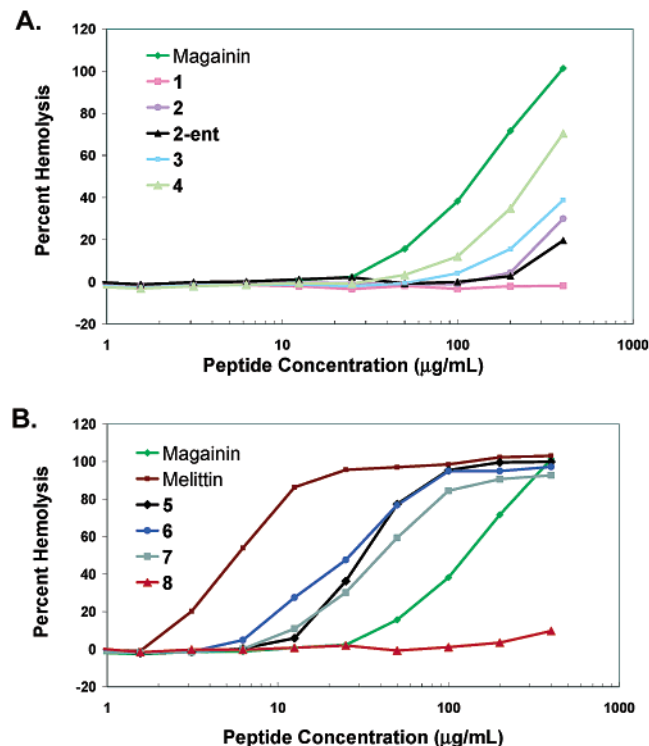


**Figure 5.** Hemolysis data for  $\beta$ -peptides 1–8 and  $\alpha$ -peptide controls. Curves are the average of at least two independent experiments with two replicates.

these antimicrobial agents to permeabilize mammalian cell membranes (Figure 5). It has been previously demonstrated that melittin is highly hemolytic,<sup>31</sup> whereas (Ala<sup>8,13,18</sup>)-magainin II amide is much less hemolytic;<sup>6,44,45</sup> therefore, these two  $\alpha$ -peptides served as controls. All  $\beta$ -peptides without N-terminal  $\beta^3$ -homotyrosine (1–4) had hemolytic activity equal to or less than that of (Ala<sup>8,13,18</sup>)-magainin II amide, while  $\beta$ -peptides 5–7, which contain an N-terminal  $\beta^3$ -homotyrosine and can form an amphiphilic structure, were more hemolytic than (Ala<sup>8,13,18</sup>)-magainin II amide. The addition of a  $\beta^3$ -homotyrosine residue to the N-terminus of 4, to generate 7, resulted in nearly an order of magnitude increase in hemolytic activity; the concentrations of  $\beta$ -peptides 4 and 7 (without and with  $\beta^3$ -homotyrosine, respectively) required to lyse 50% of the hRBC were 200–400  $\mu\text{g/mL}$  and 25–50  $\mu\text{g/mL}$ , respectively. In contrast to the results for antimicrobial activity, hemolytic activity changed little upon replacement of the free carboxyl C-terminus in 1 with a C-terminal amide ( $\beta$ -peptide 2). As expected, enantiomeric  $\beta$ -peptides 2 and 2-ent had very similar abilities to lyse hRBC. Among  $\beta$ -peptides 2–4, the hemolytic activity appeared to increase slightly with 14-helical propensity in aqueous solution, but this same trend was not seen among 5–7. As expected, nonamphiphilic 8 had negligible hemolytic activity, indicating that the ability to form an amphiphilic structure is necessary (but not sufficient) for the lysis of hRBC.

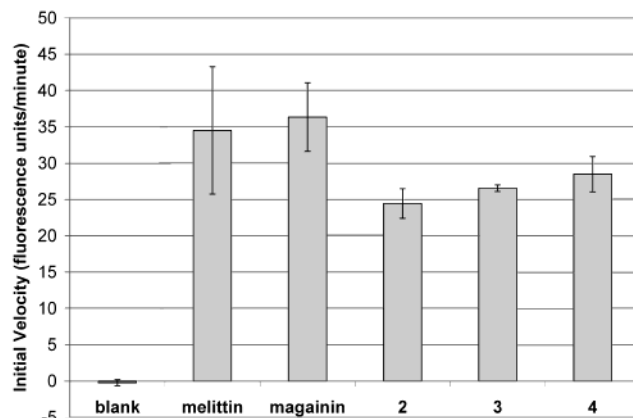


**Figure 6.** Initial velocities of the cleavage of 4-methylumbelliferyl  $\beta$ -galactoside (MUG) by  $\beta$ -galactosidase leaked from *B. subtilis* cells after incubation with  $\beta$ -peptides or controls. Initial velocities are expected to be proportional to peptide-induced leakage of functional  $\beta$ -galactosidase from bacterial cells. Error bars represent the average of at least two measurements  $\pm$  the standard deviation.

#### Peptide-Induced $\beta$ -Galactosidase Leakage from *B. subtilis*.

Peptide-induced permeabilization of *B. subtilis* BAU102<sup>60</sup> was examined by measuring *E. coli*  $\beta$ -galactosidase ( $\beta$ -gal) synthesized by *lacZ* integrated into the chromosome at the *amiE* locus, as described.<sup>60</sup> The chromosomal insertion was previously selected first on the basis of chloramphenicol resistance present in the plasmid construct used for insertion of *lacZ* and then on the basis of erythromycin resistance introduced on a second plasmid carrying *vanRS*, positive regulators of the *vanH* promoter driving *lacZ*.<sup>60</sup> *B. subtilis* BAU102 cells produce a high basal level of  $\beta$ -gal in the absence of induction of *vanRS*, which makes the peptide-induced leakage assay possible. Each initial velocity in Figure 6 is proportional to the concentration of functional  $\beta$ -gal that escaped from the cells after incubation of BAU102 with an  $\alpha$ - or  $\beta$ -peptide at a concentration well above that peptide's MIC. The  $\beta$ -gal activities observed after treatment with  $\beta$ -peptides 2–4 were indistinguishable from one another and from the control peptide melittin, within experimental uncertainty. The other positive control, (Ala<sup>8,13,18</sup>)-magainin II amide, led to  $\beta$ -gal release slightly greater than that induced by  $\beta$ -peptides 2–4. There is substantial evidence that (Ala<sup>8,13,18</sup>)-magainin II amide and melittin derive their antimicrobial activity from their ability to permeabilize bacterial membranes.<sup>9,10</sup> The similar extents of  $\beta$ -gal leakage caused by melittin, (Ala<sup>8,13,18</sup>)-magainin II amide, and  $\beta$ -peptides 2–4 suggests that these  $\beta$ -peptides also act via permeabilization of bacterial membranes.

**Lipophilicity Determination via RP-HPLC.** RP-HPLC has been used to measure the lipophilicity of various molecules,<sup>61</sup> including  $\alpha$ -helical  $\alpha$ -peptides.<sup>62</sup> We used this approach to analyze our  $\beta$ -peptides. The percent acetonitrile required to elute

(60) Ulijasz, A. T.; Grenader, A.; Weisblum, B. J. *Bacteriol.* **1996**, *178*, 6305–6309.

**Table 3.** Percent Solvent B (Acetonitrile) Required to Elute  $\beta$ -Peptides from a C4 Analytical Column<sup>a</sup>

$\beta$ -peptide	percent solvent B
<b>1</b>	37.0
<b>2</b>	35.5
<b>2-ent</b>	35.5
<b>3</b>	37.5
<b>4</b>	37.8
<b>5</b>	39.4
<b>6</b>	41.4
<b>7</b>	39.1
<b>8</b>	25.7

<sup>a</sup> Experiments were performed as described in the Materials and Methods Section. All values are the average of at least two independent experiments. The standard deviation in all cases was less than 0.4% solvent B.

each  $\beta$ -peptide from a C4 analytical column is listed in Table 3. A significantly higher percent acetonitrile was required to elute  $\beta$ -peptide **7**, which can form an amphiphilic 14-helix, than to elute isomeric **8**, which cannot form an amphiphilic 14-helix. This difference is expected, since **7** displays a much larger continuous hydrophobic surface in its 14-helical conformation than does **8**, and the difference provides a benchmark for  $\beta$ -peptides that differ significantly in lipophilicity. All other variations in elution properties among our  $\beta$ -peptides are small in comparison to **7** versus **8**, indicating that, with the exception of **8**, all  $\beta$ -peptides we examined have very similar lipophilicities. Differences are small among **2–4** and among **5–7**, the two series in which hydrophobic acyclic residues are incrementally replaced by ACHC. As expected, enantiomeric  $\beta$ -peptides **2** and **2-ent** had identical retention times.

## Discussion

We have examined  $\beta$ -peptides related to **1-ent**, previously reported by Hamuro et al.,<sup>11</sup> to evaluate systematically the relationship between 14-helical stability and biological activity. We were able to vary 14-helical propensity, as monitored by CD in aqueous solution, while keeping constant other factors believed to be important for determining biological activity, such as size, net charge, net hydrophobicity, amphiphilicity, and the widths of the hydrophobic and hydrophilic helix faces.<sup>10</sup> The antimicrobial activity we observed for **1-ent** itself (data not shown) is similar to that reported.<sup>11</sup> The hemolytic activity of **1-ent** (data not shown) is in agreement with trends in activity reported for  $\beta$ -peptides containing  $\beta^3$ -homovaline- $\beta^3$ -homolysine- $\beta^3$ -homoleucine triad repeats.<sup>11,13,63</sup> Our results for **1-ent** are also in line with those reported by Arvidsson et al.<sup>15</sup> for a similar nonamer containing a  $\beta^3$ -homoalanine- $\beta^3$ -homolysine- $\beta^3$ -homophenylalanine triad repeat.

We believe that the structure–activity relationships determined for 14-helical  $\beta$ -peptides are relevant to  $\alpha$ -helical

$\alpha$ -peptides such as the magainins because both types of peptides appear to have similar mechanisms of action. A large body of evidence suggests that  $\alpha$ -helical  $\alpha$ -peptides derive their antimicrobial properties from their ability to permeabilize bacterial membranes,<sup>64–66</sup> although evidence to the contrary has been reported in a few systems.<sup>36,67</sup> Several alternative mechanisms of membrane permeabilization have been proposed, including the formation of barrel-stave<sup>68,69</sup> or toroidal<sup>70–73</sup> pores or membrane disruption through a carpet mechanism.<sup>65</sup> More recently, other mechanisms of membrane disruption have been proposed, such as the fusion of the cell wall and cell membrane of Gram-negative bacteria.<sup>74</sup> We find that  $\beta$ -peptides **2–4** have nearly the same ability as (Ala<sup>8,13,18</sup>)-magainin II amide and melittin to permeabilize the membrane of *B. subtilis* BAU102, as measured by  $\beta$ -gal release (Figure 6). It is unlikely that these  $\beta$ -peptides derive their potency from interactions with a single chiral receptor, since enantiomeric  $\beta$ -peptides **2** and **2-ent** have nearly identical antimicrobial activities (Table 1).

Most antimicrobial  $\alpha$ -helical  $\alpha$ -peptides require the ability to form an amphiphilic helix for activity,<sup>10</sup> although Oren and Shai have found that peptides containing one-third D residues and end-to-end cyclization are active despite the low probability of  $\alpha$ -helix formation.<sup>37</sup> A requirement for amphiphilic helix formation among our  $\beta$ -peptides is indicated by the observation that **8** is much less active than isomer **7**. Our  $\beta$ -peptides probably cannot span bacterial membranes (ca. 30 Å wide) because the 14-helices formed by nine- or ten-residue  $\beta$ -peptides such as **1–8** should be only approximately 15 Å long. Therefore, it is unlikely that these  $\beta$ -peptides permeabilize bacterial membranes via the barrel-stave mechanism, unless the helices align end-to-end during transmembrane pore formation. The barrel-stave mechanism is also unlikely for **2–4** because these  $\beta$ -peptides are more potent in lysing bacterial cells relative to human red blood cells; cell selectivity is less common with the barrel-stave mode of action than with the carpet or toroidal pore mechanisms.<sup>10</sup> Analysis of interactions between these  $\beta$ -peptides and liposomes is underway.<sup>75</sup>

Replacement of the C-terminal carboxylic acid in **1** with a primary amide (**2**) results in a one to two orders of magnitude increase in antimicrobial activity against all four strains of bacteria. The higher potency of **2** most likely results from an increase in the net positive charge of **2**, relative to **1**, which enhances electrostatic attraction to the negatively charged phospholipids in bacterial membranes. Likewise, the C-terminal amide forms of the magainins,<sup>42</sup> cecropin A,<sup>43</sup> and a melittin diastereomer<sup>35</sup> were also found to be more active than the

- (61) Du, C. M.; Valko, K.; Bevan, C.; Reynolds, D.; Abraham, M. H. *Anal. Chem.* **1998**, *70*, 4228–4234.  
 (62) Wagschal, K.; Triplet, B.; Lavigne, P.; Mant, C.; Hodges, R. S. *Protein Sci.* **1999**, *8*, 2312–2329.  
 (63) Reference 13 states that the  $\beta$ -peptide H-( $\beta^3$ -homovaline- $\beta^3$ -homolysine- $\beta^3$ -homoleucine)<sub>4</sub>-OH reported originally in ref 11 had been contaminated with the Fmoc-protected  $\beta$ -peptide dodecamer. Although the presence of the impurity did not significantly affect antimicrobial activity, elimination of the impurity resulted in a 10-fold decrease in hemolytic activity.<sup>11,13</sup> We infer that the analogous  $\beta$ -peptide reported in ref 11, H-( $\beta^3$ -homovaline- $\beta^3$ -homolysine- $\beta^3$ -homoleucine)<sub>3</sub>-OH (**1-ent**, here), was also contaminated with the Fmoc-protected impurity. In the series Fmoc-( $\beta^3$ -homovaline- $\beta^3$ -homolysine- $\beta^3$ -homoleucine)<sub>n</sub>-OH, the elimination of one triad of residues resulted in a 20-fold increase in the HC<sub>50</sub>.<sup>11</sup> By analogy, we expect the HC<sub>50</sub> of a pure sample of the  $\beta$ -peptide H-( $\beta^3$ -homovaline- $\beta^3$ -homolysine- $\beta^3$ -homoleucine)<sub>n</sub>-OH (where  $n = 3$ ) will be approximately 800  $\mu$ M, 20-fold higher than that of  $n = 4$  (37  $\mu$ M<sup>13</sup>).

- (64) Bechinger, B. *Biochim. Biophys. Acta* **1999**, *1462*, 157–183.  
 (65) Oren, Z.; Shai, Y. *Biopolymers* **1998**, *47*, 451–463.  
 (66) Huang, H. W. *Biochemistry* **2000**, *39*, 8347–8352.  
 (67) Zhang, L.; Rozek, A.; Hancock, R. E. W. *J. Biol. Chem.* **2001**, *276*, 35714–35722.  
 (68) Christensen, B.; Fink, J.; Merrifield, R. B.; Mauzerall, D. *Proc. Natl. Acad. Sci. U.S.A.* **1988**, *85*, 5072–5076.  
 (69) Merrifield, R. B.; Merrifield, E. L.; Juvvadi, P.; Andreu, D.; Boman, H. G. *Ciba Found Symp.* **1994**, *186*, 5–20.  
 (70) Luttkie, S.; He, K.; Huang, H. *Biochemistry* **1995**, *34*, 16764–16769.  
 (71) Luttkie, S. J.; He, K.; Heller, W. T.; Harroun, T. A.; Yang, L.; Huang, H. W. *Biochemistry* **1996**, *35*, 13723–13728.  
 (72) Matsuzaki, K.; Murase, O.; Fujii, N.; Miyajima, K. *Biochemistry* **1996**, *35*, 11361–11368.  
 (73) Matsuzaki, K.; Murase, O.; Fujii, N.; Miyajima, K. *Biochemistry* **1995**, *34*, 6521–6526.  
 (74) Liechty, A.; Chen, J.; Jain, M. K. *Biochim. Biophys. Acta* **2000**, *1463*, 55–64.  
 (75) Epan, R. F.; Raguse, T. L.; Gellman, S. H.; Epan, R. M. Manuscript in preparation.



corresponding carboxylic acids. C-terminal amidation of  $\alpha$ -peptides stabilizes the  $\alpha$ -helical conformation through favorable interactions with the helix dipole<sup>76,77</sup> and the potential for an additional hydrogen bond. In contrast, C-terminal amidation of the  $\beta$ -peptides described here should destabilize the 14-helical structure through unfavorable interactions with the helix dipole (the helix dipole of 14-helical  $\beta$ -peptides runs from C-terminus to N-terminus, in contrast to the N-to-C dipole of  $\alpha$ -helical  $\alpha$ -peptides).

Several groups have evaluated the antimicrobial activities of  $\alpha$ -peptides that display variable extents of  $\alpha$ -helix formation in mixed aqueous/organic solvents, which are proposed to represent membrane-like environments;<sup>32</sup> these  $\alpha$ -peptides are unstructured in aqueous solution.<sup>31,33,34,36</sup> In most cases, increased  $\alpha$ -helical population in mixed aqueous/organic solvents correlates with higher antimicrobial activity.<sup>31,33,36</sup> However, Shai and Oren noted that the introduction of three D-amino acid residues into the toxin paradaxin had little effect on antimicrobial activity, even though the extent of  $\alpha$ -helix population in aqueous TFE was greatly reduced by the D residues.<sup>34</sup> In contrast, Houston and co-workers determined that increasing  $\alpha$ -helical stability in aqueous solution through the formation of lactam bridges decreases antimicrobial activity; in most cases, the creation of the lactam bridge appeared, from CD analysis, to have no effect on  $\alpha$ -helical stability in aqueous TFE.<sup>32</sup>

We have shown that increasing the 14-helical propensity of  $\beta$ -peptides has little effect on antimicrobial activity. The amount of 14-helical structure in aqueous solution (Figure 2) varies from  $\sim 0\%$  to  $\sim 100\%$  within the two series of  $\beta$ -peptides, **2–4** and **5–7**, but there is no consistent relationship between 14-helical stability and MIC values (Table 1) outside the limits of experimental uncertainty. In contrast, the identity of the C-terminal group (**1** versus **2**) and the ability of the  $\beta$ -peptide to form an amphiphilic helix as opposed to a nonamphiphilic helix (**7** versus **8**) are crucial for activity.

At first glance, our results appear to contradict the conclusions of Houston et al., who proposed that stabilizing the  $\alpha$ -helical conformation among  $\alpha$ -peptides leads to a decrease in antibacterial activity.<sup>32</sup> However, the range of helical stability in aqueous solution among our  $\beta$ -peptides was much greater than among the  $\alpha$ -peptides examined by Houston et al.  $\beta$ -Peptide structuring in aqueous solution varied from no detectable 14-helical structure to almost entirely 14-helical. In contrast, Houston et al. reported much smaller differences in  $\alpha$ -helical structure in aqueous solution: increases of 16 to 66% or 8 to 37% upon formation of a lactam bridge. The only bacteria common to both studies was *E. coli*. For Houston's  $\alpha$ -peptide analogues with the largest increase in helical structure upon formation of the lactam bridge (16 to 66%), the MIC against *E. coli* decreased only by a factor of two for the bridged peptide, which is within experimental uncertainty in our hands.

Increased  $\alpha$ -helical propensity in mixed aqueous/organic solvents seems to correlate with increased lysis of hRBC by antimicrobial  $\alpha$ -peptides, especially when the barrel-stave mechanism is the mode of membrane permeabilization.<sup>33–35</sup> However, it was previously unknown how preformation of

helical structure in aqueous solution would affect lysis of hRBC by helical peptides. We find that the amount of 14-helical structure in aqueous solution is not related to the ability of  $\beta$ -peptides to lyse hRBC.  $\beta$ -Peptides **5–7** have very similar hemolytic activities (Figure 5) despite their very different 14-helix populations in aqueous solution (Figure 2B). Hemolytic activity appears to increase marginally with the amount of 14-helical structure in aqueous solution among  $\beta$ -peptides **2–4**, but higher hemolytic activity in this series may also result from very subtle increases in lipophilicity (Table 3). The addition of a hydrophobic N-terminal  $\beta^3$ -homotyrosine increases hemolytic activity by approximately an order of magnitude (**4** versus **7**). DeGrado and co-workers<sup>11,13</sup> have obtained similar results; they reported a 100-fold increase in hemolytic activity upon addition of a hydrophobic Fmoc protecting group to the amino-terminus of H-( $\beta^3$ -homovaline- $\beta^3$ -homolysine- $\beta^3$ -homoleucine)<sub>4</sub>-OH.

Neither antimicrobial activity nor hemolytic activity increases significantly among our  $\beta$ -peptides when 14-helical propensity is substantially increased. In contrast, stronger affinity of peptide and peptidomimetic ligands to specific proteins is often observed when the ligand is rigidified to favor the binding conformation.<sup>78</sup> Cell membranes appear to be the biologically relevant binding partners of the antimicrobial  $\beta$ -peptides. The lack of correlation between the extent of 14-helix formation in aqueous solution and either antimicrobial or hemolytic activity suggests that the loss of conformational entropy upon binding of unfolded  $\beta$ -peptides to cell membranes is relatively modest.

We have used the unique structural properties of  $\beta$ -peptides to determine whether the stability of the biologically active conformation influences antibacterial or hemolytic activity. We conclude that variation over a broad range of helical propensity has little effect on either activity. In contrast, some other workers have concluded that helix propensity among  $\alpha$ -peptides has a substantial effect on antimicrobial activity<sup>31–33,36</sup> and hemolytic activity.<sup>33–36</sup> In most of those studies, structural analysis was conducted in mixed aqueous/organic solvents,<sup>31–36</sup> while we were able to analyze  $\beta$ -peptide folding in water. We believe that our results are relevant to the behavior of  $\alpha$ -peptides because of mechanistic similarities between these two peptide classes (both permeabilize bacterial membranes). This study suggests that  $\beta$ -peptides capable of mimicking other  $\alpha$ -peptide functions will prove useful for elucidating the dependence of these functions on conformational stability.

## Materials and Methods

**General Procedures.** Proton nuclear magnetic resonance (<sup>1</sup>H NMR) spectra were recorded in deuterated solvents on a Bruker AC-300 (300 MHz) spectrometer. Chemical shifts are reported in parts per million (ppm,  $\delta$ ) relative to tetramethylsilane ( $\delta$  0.00). Matrix-assisted laser desorption–ionization time-of-flight mass spectra (MALDI-TOF-MS) were obtained on a Bruker REFLEX II spectrometer with a 337-nm laser using the  $\alpha$ -cyano-4-hydroxycinnamic acid matrix. The instrument was calibrated to a standard mixture of leu<sup>5</sup>-enkephalin ( $M + H^+ = 556.28$ ), angiotensin I ( $M + H^+ = 1296.7$ ), and neurotensin ( $M + H^+ = 1672.9$ ). Optical rotation was measured using sodium light (D line, 589.3 nm).

**Materials.** CH<sub>2</sub>Cl<sub>2</sub> was distilled from CaH<sub>2</sub>. Hexane was distilled. DMF for manual solid-phase peptide synthesis was purchased from Aldrich (HPLC grade) and stored over Dowex 50W-X8 ion-exchange resin. Ether was anhydrous. The highest available grade of all other

(76) Shoemaker, K. R.; Kim, P. S.; Brems, D. N.; Marqusee, S.; York, E. J.; Chaiken, I. M.; Stewart, J. M.; Baldwin, R. L. *Proc. Natl. Acad. Sci. U.S.A.* **1985**, *82*, 2349–2353.

(77) Shoemaker, K. R.; Kim, P. S.; York, E. J.; Stewart, J. M.; Baldwin, R. L. *Nature* **1987**, *326*, 563–567.

(78) Babine, R. E.; Bender, S. L. *Chem. Rev.* **1997**, *97*, 1359–1472.

solvents was purchased and used without further purification. Diisopropylethylamine (DIEA) was distilled from  $\text{CaH}_2$ .  $\text{H}_2\text{O}_2$  was purchased from Mallinckrodt, and 4 N HCl in dioxane was obtained from Pierce. Wang resin (p-benzyloxybenzyl alcohol resin; loading = 0.75 mmol/g) and 9-fluorenylmethylxycarbonyl-N-hydroxysuccinimide (Fmoc-OSu) were purchased from Novabiochem. Fmoc amide resin [4-(2',4'-dimethoxyphenyl-Fmoc-aminomethyl)phenoxyacetamido-ethyl resin; polystyrene resin functionalized with a Knorr linker; loading = 0.63 mmol/g] was obtained from Applied Biosystems. (Ala<sup>8,13,18</sup>)-Magainin II amide, melittin, 4-methylumbelliferyl  $\beta$ -D-galactoside (MUG), and TRIS were purchased from Sigma. All other reagents were purchased from Aldrich.

Analytical thin-layer chromatography (TLC) was carried out on Whatman TLC plates precoated with silica gel 60 (250- $\mu\text{m}$  layer thickness). Solvent mixtures used for TLC are reported in v/v ratios. Sterile Falcon 3075 microtiter 96-well plates were used for biological assays.  $\beta$ -Peptides were purified by RP-HPLC on a Vydac C4 semiprep column using a flow rate of 3 mL/min. Solvent A and solvent B for RP-HPLC were 0.045% TFA in Millipore water and 0.036% TFA in acetonitrile, respectively.  $\beta$ -Peptide purity was assessed using a linear gradient of 5–95% solvent B over 57 min on a Vydac C4 analytical column, monitoring at 220 nm. The purity of each  $\beta$ -peptide after RP-HPLC was greater than 95%.

**Synthesis of  $\beta$ -Amino Acid Monomers.** Fmoc-protected acyclic  $\beta$ -amino acid monomers were synthesized as described previously.<sup>46,47</sup> Boc-*trans*-2-aminocyclohexanecarboxylic acid (Boc-ACHC-OMe)<sup>41</sup> was converted to Fmoc-ACHC-OH as described below.

**Boc-ACHC-OH.** Methanol (105 mL) and Millipore water (35 mL) were added to Boc-ACHC-OMe<sup>41</sup> (1.83 g, 7.12 mmol), followed by  $\text{LiOH}\cdot\text{H}_2\text{O}$  (3.58 g, 85.4 mmol) and 26%  $\text{H}_2\text{O}_2$  in water (4.66 mL, 35.6 mmol). The mixture was stirred at room temperature for 36 h. A solution of  $\text{Na}_2\text{SO}_3$  (13.4 g, 106 mmol) in Millipore water (80 mL) was then added at 0 °C, and the mixture was stirred for 10 min. The methanol was removed by rotary evaporation. The aqueous solution was cooled to 0 °C and acidified with 3 M HCl until white solid precipitated. This mixture was treated with ethyl acetate, which caused the precipitate to dissolve, and the layers were separated. The aqueous layer was further acidified to pH 2 with 3 M HCl and re-extracted with the same ethyl acetate and then with four additional aliquots ethyl acetate. The organic extracts were combined, dried over  $\text{MgSO}_4$ , concentrated, and dried in vacuo to yield 1.68 g Boc-ACHC-OH (97% yield) as a white solid. The <sup>1</sup>H NMR spectrum was identical to the published spectrum of Boc-ACHC-OH.<sup>23</sup>

**Fmoc-ACHC-OH.** A solution of 4 N HCl in dioxane (40 mL) was added to Boc-ACHC-OH (1.68 g, 6.91 mmol), and after a few min a white solid precipitated from the clear solution. The mixture was stirred at room temperature for 1 h, and then the solvent was removed under a stream of  $\text{N}_2$ . The white solid was dried under vacuum.  $\text{CH}_3\text{CN}$  (66 mL) and Millipore water (17 mL) were added, followed by DIEA (3.57 mL, 20.1 mmol) and Fmoc-OSu (2.26 g, 6.70 mmol). The mixture was stirred at room temperature for 30 min or until TLC showed that the Fmoc-OSu was almost completely consumed ( $R_f = 0.45$  in 1:1 hexane/ethyl acetate). The pH was neutralized with aqueous 1 M HCl at 0 °C and the  $\text{CH}_3\text{CN}$  was removed by rotary evaporation. More 1 M HCl was added at 0 °C until the pH was equal to 2 and white solid precipitated. The white solid was collected via suction filtration and washed with dilute HCl solution. The product was dissolved in ethyl acetate and washed with 1 M HCl and with brine. The organic layer was dried over  $\text{MgSO}_4$  and concentrated in vacuo. The product was recrystallized from hexane/ethyl acetate to afford 2.17 g Fmoc-ACHC-OH (86% yield) as a fluffy white solid: mp 200–201 °C;  $[\alpha]_D^{25} = -37.9$  ( $c$  0.5, acetone); IR (thin film) 3310 (NH), 1694 (C=O),  $\text{cm}^{-1}$ ; <sup>1</sup>H NMR ( $\text{CDCl}_3 + \text{CD}_3\text{OD}$ , 300 MHz):  $\delta$  7.77 (d,  $J = 7.3$  Hz, 2H), 7.62 (d,  $J = 7.0$  Hz, 2H), 7.44–7.28 (m, 4H), 4.50–4.18 (m, 3H), 3.77–3.48 (m, 1H), 2.36–2.13 (m, 1H), 2.07–1.92 (m, 2H), 1.82–

1.01 (m, 6H); FAB-MS  $m/z$  calcd for  $\text{C}_{22}\text{H}_{23}\text{NO}_4\text{Na}$  ( $M + \text{Na}^+$ ) 388.1525, obsd 388.1517.

**Synthesis of  $\beta$ -Peptides. General Procedures for Solid-Phase Synthesis.**  $\beta$ -Peptides were synthesized on Fmoc amide resin (25- $\mu\text{mol}$  scale) on an Applied Biosystems Model 432A (Synergy) automated peptide synthesizer using standard Fmoc/*t*-Bu strategy with *O*-benzotriazol-1-yl-*N,N,N,N'*-tetramethyluronium hexafluorophosphate (HBTU) and 1-hydroxybenzotriazole (HOBt) as coupling reagents unless stated otherwise. Two-hour coupling times were employed. The program module controlling Fmoc deprotection was modified to extend the deprotection time automatically, if necessary. Cleavage from the resin and simultaneous deprotection of the side chain protecting groups were accomplished with 2,2,2-trifluoroacetic acid (TFA) via one of the procedures described below. After purification via RP-HPLC, each  $\beta$ -peptide was lyophilized. Freshly lyophilized  $\beta$ -peptides were dissolved in Millipore water to create 2 mg/mL  $\beta$ -peptide solutions that were stored at –78 °C.

**Combined Automated/Manual Synthesis of Difficult Sequences.** It was necessary to perform certain deprotection steps manually during the synthesis of  $\beta$ -peptides **3** and **6** to attain the high temperatures necessary for complete removal of the Fmoc-protecting group. For convenience, each coupling step between two high-temperature deprotections was performed manually. The peptide-resin (25  $\mu\text{mol}$ ) was removed from the automated peptide synthesizer and washed with DMF (3  $\times$  1 min),  $\text{Et}_2\text{O}$  (3  $\times$  1 min),  $\text{CH}_2\text{Cl}_2$  (3  $\times$  1 min), and NMP (3  $\times$  1 min). The resin was transferred to a glass centrifuge tube and deprotected with 20% piperidine in NMP at 60 °C, with mixing via nitrogen bubbling, for 1 h. After cooling to room temperature, the mixture was transferred to a fritted reaction vessel. The resin was isolated by filtration and washed with NMP (3  $\times$  1 min),  $\text{Et}_2\text{O}$  (3  $\times$  1 min),  $\text{CH}_2\text{Cl}_2$  (3  $\times$  1 min) and DMF (3  $\times$  1 min). The next  $\beta$ -amino acid was coupled by adding HOBt (150  $\mu\text{L}$  of a 0.5 M solution in DMF, 75  $\mu\text{mol}$ ), DIEA (300  $\mu\text{L}$  of a 0.5 M solution in DMF, 150  $\mu\text{mol}$ ),  $\text{CH}_2\text{Cl}_2$  (450  $\mu\text{L}$ ), the appropriate Fmoc- $\beta$ -amino acid (75  $\mu\text{mol}$  freshly dissolved in 600  $\mu\text{L}$  DMF), and benzotriazol-1-yloxytripyrroli-dinophosphonium hexafluorophosphate (PyBOP) (39.0 mg, 75  $\mu\text{mol}$  freshly dissolved in 600  $\mu\text{L}$  DMF) to the peptide-resin. The mixture was agitated for 8 h. The resin was isolated by filtration and washed with DMF (3  $\times$  1 min),  $\text{Et}_2\text{O}$  (3  $\times$  1 min), and  $\text{CH}_2\text{Cl}_2$  (3  $\times$  1 min). Remaining free amines were capped by adding a solution of acetic anhydride (84  $\mu\text{L}$ , 890  $\mu\text{mol}$ ) and DIEA (84  $\mu\text{L}$ , 480  $\mu\text{mol}$ ) in  $\text{CH}_2\text{Cl}_2$  (2 mL) to the resin and agitating for 1 h. The resin was isolated by filtration and washed with  $\text{CH}_2\text{Cl}_2$  (3  $\times$  1 min),  $\text{Et}_2\text{O}$  (3  $\times$  1 min),  $\text{CH}_2\text{Cl}_2$  (3  $\times$  1 min), and NMP (3  $\times$  1 min). The resin was transferred to a glass centrifuge tube and deprotected with 20% piperidine in NMP at 60 °C, with mixing via nitrogen bubbling, for 1 h. After cooling to room temperature, the resin was washed with NMP (3  $\times$  1 min),  $\text{Et}_2\text{O}$  (3  $\times$  1 min), and  $\text{CH}_2\text{Cl}_2$  (3  $\times$  1 min). Synthesis was continued on the automated peptide synthesizer.

**Cleavage from Resin and Side Chain Deprotection. Procedure A.** The peptide was cleaved from the resin with 95:5 TFA: $\text{H}_2\text{O}$  (8 mL) for 3 h. The resin was removed via filtration through cotton and rinsed with additional TFA. The combined filtrate was concentrated under a stream of nitrogen.

**Procedure B.** The peptide was cleaved from the resin with 95:2.5:2.5 TFA:ethanedithiol: $\text{H}_2\text{O}$  (8 mL) for 3 h. The resin was removed via filtration through glass wool and rinsed with additional TFA. The combined filtrate was concentrated under a stream of nitrogen. A minimal amount of methanol was added to dissolve the crude  $\beta$ -peptide, and  $\text{Et}_2\text{O}$  (10 mL) was added to form a white precipitate. The mixture was cooled in an acetone/dry ice bath for 5 min, centrifuged, and the  $\text{Et}_2\text{O}$  was decanted from the white pellet. A new portion of  $\text{Et}_2\text{O}$  (10 mL) was added, the mixture was stirred with a spatula, cooled in an acetone/dry ice bath for 5 min, and centrifuged, and the  $\text{Et}_2\text{O}$  was decanted from the white pellet. Any  $\text{Et}_2\text{O}$  remaining with the white solid was evaporated under a gentle stream of nitrogen.

**$\beta$ -Peptide 1.** Fmoc- $\beta^3$ -homoleucine-OH<sup>44</sup> was manually loaded onto the resin via the procedure given below. Wang resin (33.3 mg, 25.0  $\mu$ mol) was washed with DMF (3  $\times$  1 min), Et<sub>2</sub>O (3  $\times$  1 min), and CH<sub>2</sub>Cl<sub>2</sub> (3  $\times$  1 min). Fmoc- $\beta^3$ -homoleucine-OH (55.1 mg, 150  $\mu$ mol) was weighed into a vial and dissolved in CH<sub>2</sub>Cl<sub>2</sub>. Diisopropyl carbodiimide (11.7  $\mu$ L, 75  $\mu$ mol) and 4-(dimethylamino)pyridine (9.2 mg, 75  $\mu$ mol) were added to the CH<sub>2</sub>Cl<sub>2</sub> solution. The CH<sub>2</sub>Cl<sub>2</sub> solution was then transferred to the vessel containing the washed resin with CH<sub>2</sub>Cl<sub>2</sub> (1.2 mL total CH<sub>2</sub>Cl<sub>2</sub>) and the mixture was agitated at room temperature for 48 h. The resin was isolated by filtration and washed with DMF (4  $\times$  1 min). Trimethylacetic anhydride (51  $\mu$ L, 250  $\mu$ mol), pyridine (20  $\mu$ L, 250  $\mu$ mol), and DMF (2 mL) were combined in a separate vial and added to the resin to cap any unreacted free hydroxyl groups. The mixture was agitated at room temperature for 1 h. The resin was isolated by filtration and washed with DMF (4  $\times$  1 min), methanol (4  $\times$  1 min), and CH<sub>2</sub>Cl<sub>2</sub> (4  $\times$  1 min). The resin was dried in vacuo. The synthesis was then continued as described under General Procedures for Solid-Phase Synthesis on the automated peptide synthesizer. The  $\beta$ -peptide was cleaved from the resin with 50% TFA in CH<sub>2</sub>Cl<sub>2</sub> (12 mL) for 1.5 h. The resin was removed via filtration through cotton and rinsed with additional 50% TFA in CH<sub>2</sub>Cl<sub>2</sub>. The combined filtrate was concentrated under a stream of nitrogen. The crude  $\beta$ -peptide was dissolved in the HPLC A solvent and purified by RP-HPLC employing a linear gradient from 25% to 45% solvent B over 40 min. MALDI-TOF-MS *m/e* calcd for (C<sub>60</sub>H<sub>116</sub>N<sub>12</sub>O<sub>10</sub>) (M) 1164.9, found 1165.7 (M + H<sup>+</sup>), 1187.7 (M + Na<sup>+</sup>), 1203.7 (M + K<sup>+</sup>), 1209.7 (M + 2Na<sup>+</sup> - H<sup>+</sup>).

**$\beta$ -Peptide 1-ent.** Synthesis and purification were performed as described for **1**. MALDI-TOF-MS *m/e* calcd for (C<sub>60</sub>H<sub>116</sub>N<sub>12</sub>O<sub>10</sub>) (M) 1164.9, found 1165.8 (M + H<sup>+</sup>), 1187.7 (M + Na<sup>+</sup>), 1203.7 (M + K<sup>+</sup>), 1209.7 (M + 2Na<sup>+</sup> - H<sup>+</sup>).

**$\beta$ -Peptide 2.** The synthesis was performed as described under General Procedures for Solid-Phase Synthesis on the automated peptide synthesizer. Cleavage of the  $\beta$ -peptide and simultaneous side chain deprotection were performed as described under Procedure A. The crude  $\beta$ -peptide was dissolved in the HPLC A solvent and purified by RP-HPLC employing a linear gradient from 26% to 41% solvent B over 30 min. MALDI-TOF-MS *m/e* calcd for (C<sub>60</sub>H<sub>117</sub>N<sub>13</sub>O<sub>9</sub>) (M) 1163.9, found 1164.7 (M + H<sup>+</sup>), 1186.8 (M + Na<sup>+</sup>), 1202.7 (M + K<sup>+</sup>).

**$\beta$ -Peptide 2-ent.** Synthesis and purification were performed as described for **2**. MALDI-TOF-MS *m/e* calcd for (C<sub>60</sub>H<sub>117</sub>N<sub>13</sub>O<sub>9</sub>) (M) 1163.9, found 1164.9 (M + H<sup>+</sup>), 1186.9 (M + Na<sup>+</sup>), 1202.8 (M + K<sup>+</sup>).

**$\beta$ -Peptide 3.** The coupling of residues 1–6 was performed as described under General Procedures for Solid-Phase Synthesis on the automated peptide synthesizer. The program module controlling the DMF rinse cycle after the 6th coupling was modified to extend the rinsing time automatically if needed to allow the conductivity level to return to baseline. Fmoc-deprotection of the 6th residue was repeated manually at 60 °C, and coupling and high-temperature deprotection of the 7th residue were also performed manually as described under Combined Automated/Manual Synthesis of Difficult Sequences. Synthesis of residues 8 and 9 were performed as described under General Procedures for Solid-Phase Synthesis on the automated peptide synthesizer, except that the final ACHC residue was double-coupled, and the program module controlling the DMF rinse cycle after each coupling was modified to extend the rinsing time automatically if needed to allow the conductivity level to return to baseline. Cleavage of the  $\beta$ -peptide and simultaneous side chain deprotection were performed as described in Procedure A. The crude  $\beta$ -peptide was dissolved in the HPLC A solvent and purified by RP-HPLC employing a linear gradient from 28% to 43% solvent B over 30 min. MALDI-TOF-MS *m/e* calcd for (C<sub>63</sub>H<sub>117</sub>N<sub>13</sub>O<sub>9</sub>) (M) 1199.9, found 1200.8 (M + H<sup>+</sup>), 1222.8 (M + Na<sup>+</sup>), 1238.8 (M + K<sup>+</sup>).

**$\beta$ -Peptide 4.** The synthesis was performed as described under General Procedures for Solid-Phase Synthesis on the automated peptide

synthesizer, except that the program module controlling the DMF rinse cycles after the 6th, 7th, and 8th couplings was modified to extend the rinsing times automatically if needed to allow the conductivity level to return to baseline. Cleavage of the  $\beta$ -peptide and simultaneous side chain deprotection were performed as described in Procedure A. The crude  $\beta$ -peptide was dissolved in the HPLC A solvent and purified by RP-HPLC employing a linear gradient from 27% to 49% solvent B over 45 min. MALDI-TOF-MS *m/e* calcd for (C<sub>63</sub>H<sub>111</sub>N<sub>13</sub>O<sub>9</sub>) (M) 1193.9, found 1194.9 (M + H<sup>+</sup>), 1216.8 (M + Na<sup>+</sup>), 1232.8 (M + K<sup>+</sup>).

**$\beta$ -Peptide 5.** The synthesis was performed as described under General Procedures for Solid-Phase Synthesis on the automated peptide synthesizer. Cleavage of the  $\beta$ -peptide and simultaneous side chain deprotection were performed as described in Procedure B. The crude  $\beta$ -peptide was dissolved in 10:1 HPLC A solvent:methanol with sonication and purified by RP-HPLC employing a linear gradient from 30% to 42.5% solvent B over 25 min. MALDI-TOF-MS *m/e* calcd for (C<sub>73</sub>H<sub>134</sub>N<sub>14</sub>O<sub>11</sub>) (M) 1383.0, found 1384.2 (M + H<sup>+</sup>), 1406.3 (M + Na<sup>+</sup>), 1422.2 (M + K<sup>+</sup>).

**$\beta$ -Peptide 6.** The coupling of residues 1–5 was performed as described under General Procedures for Solid-Phase Synthesis on the automated peptide synthesizer, except that the program module controlling the DMF rinse cycles after each coupling was modified to extend the rinsing time automatically if needed to allow the conductivity level to return to baseline. Fmoc-deprotection of the 5th residue was repeated manually at 60 °C, and coupling and high-temperature deprotection of the 6th residue were also performed manually as described under Combined Automated/Manual Synthesis of Difficult Sequences. Synthesis of residues 7–10 was performed as described under General Procedures for Solid-Phase Synthesis on the automated peptide synthesizer, except that the final ACHC residue was double-coupled, and the program module controlling the DMF rinse cycles after each coupling was modified to extend the rinsing time automatically if needed to allow the conductivity level to return to baseline. Cleavage of the  $\beta$ -peptide and simultaneous side chain deprotection were performed as described in Procedure B. The crude  $\beta$ -peptide was dissolved in the HPLC A solvent and purified by RP-HPLC employing a linear gradient from 30% to 50% solvent B over 40 min. MALDI-TOF-MS *m/e* calcd for (C<sub>73</sub>H<sub>128</sub>N<sub>14</sub>O<sub>11</sub>) (M) 1377.0, found 1377.9 (M + H<sup>+</sup>), 1399.9 (M + Na<sup>+</sup>), 1415.9 (M + K<sup>+</sup>).

**$\beta$ -Peptide 7.** The synthesis was performed as described under General Procedures for Solid-Phase Synthesis on the automated peptide synthesizer, except that the program module controlling the DMF rinse cycles after each coupling was modified to extend the rinsing time automatically if needed to allow the conductivity level to return to baseline. The final three ACHC residues were double-coupled. Cleavage of the  $\beta$ -peptide and simultaneous side chain deprotection were performed as described in Procedure B. The crude  $\beta$ -peptide was dissolved in the HPLC A solvent and purified by RP-HPLC employing a linear gradient from 30% to 42.5% solvent B over 25 min. MALDI-TOF-MS *m/e* calcd for (C<sub>73</sub>H<sub>122</sub>N<sub>14</sub>O<sub>11</sub>) (M) 1370.9, found 1371.7 (M + H<sup>+</sup>), 1393.7 (M + Na<sup>+</sup>), 1409.7 (M + K<sup>+</sup>).

**$\beta$ -Peptide 8.** The synthesis was performed as described under General Procedures for Solid-Phase Synthesis on the automated peptide synthesizer, except that each ACHC residue was double-coupled, and the program module controlling the DMF rinse cycle after each coupling was modified to extend the rinsing time automatically if needed to allow the conductivity level to return to baseline. Cleavage of the  $\beta$ -peptide and simultaneous side chain deprotection were performed as described in Procedure B. The crude  $\beta$ -peptide was dissolved in the HPLC A solvent and purified by RP-HPLC employing a linear gradient from 17% to 30% solvent B over 25 min. MALDI-TOF-MS *m/e* calcd for (C<sub>73</sub>H<sub>122</sub>N<sub>14</sub>O<sub>11</sub>) (M) 1370.9, found 1371.7 (M + H<sup>+</sup>), 1393.7 (M + Na<sup>+</sup>), 1409.7 (M + K<sup>+</sup>).

**Circular Dichroism.** A 2 mg/mL stock solution of each  $\beta$ -peptide in Millipore water (concentration determined by mass of freshly

lyophilized  $\beta$ -peptide as its TFA salt, assuming one TFA counterion per amine) was combined with aqueous TRIS-buffered saline to give aqueous solutions of 0.2 mg/mL  $\beta$ -peptide in 10 mM TRIS, 150 mM NaCl, pH 7.2. Alternatively, each 2 mg/mL stock solution of  $\beta$ -peptide in Millipore water was combined with aqueous TRIS-buffered saline and TFE to give solutions of 0.2 mg/mL  $\beta$ -peptide, 4.4 mM TRIS, and 67 mM NaCl in 60% aqueous TFE. The final concentration of  $\beta$ -peptides **5–8** in each aqueous TRIS-buffered saline solution was determined by the UV absorbance of that solution (UV absorbance was measured immediately after obtaining the CD spectrum), whereas the final concentration of  $\beta$ -peptide in each 60% TFE solution was calculated from the UV absorbance of the 2 mg/mL stock solution. We assume the extinction coefficient of each  $\beta$ -peptide is  $1420 \text{ cm}^{-1} \text{ M}^{-1}$  at 275 nm, the extinction coefficient of  $\alpha$ -tyrosine.<sup>79</sup> The concentration determined by mass was within 80% of the concentration determined by UV absorbance for each  $\beta$ -peptide solution. Circular dichroism spectra were obtained on an Aviv 202SF spectrometer at room temperature with 1-mm path length cells and 10-s averaging times. The CD signal of the corresponding buffer solution was subtracted from the CD spectrum of each  $\beta$ -peptide solution. Data were converted to ellipticity ( $\text{deg cm}^2 \text{ dmol}^{-1}$ ) according to the equation:

$$[\Theta] = \psi M_l / 100lc$$

where  $\psi$  is the CD signal in degrees,  $M_l$  is the molecular weight divided by the number of residues,  $l$  is the path length in decimeters, and  $c$  is the concentration in grams per milliliter.

**TFE Titration.** Aliquots (40  $\mu\text{L}$  each) of a 2 mg/mL stock solution of **2** were combined with 360  $\mu\text{L}$  TRIS-buffered saline (11.1 mM TRIS + 167 mM NaCl, pH 7.2) and TFE in varying proportions. The CD spectra of the resulting 0.2 mg/mL solutions of **2** were obtained as described above.

**Minimal Inhibitory Concentration Determination.** The bacteria used for these experiments were *Escherichia coli* JM109,<sup>59</sup> *Bacillus subtilis* BR151,<sup>56</sup> *Enterococcus faecium* A634 (vancomycin resistant),<sup>58</sup> and *Staphylococcus aureus* 1206 (penicillin resistant).<sup>57</sup> Cells were grown overnight in brain–heart infusion (BHI) medium (37 g Difco brain–heart infusion dissolved in 1 L water) at 37 °C to a final concentration of approximately  $10^8$  colony forming units/mL. Cells were diluted to a concentration of  $10^7$  colony forming units/mL with sterile BHI medium, determined by the absorbance, and then diluted 20-fold with sterile BHI medium. Two-fold serial dilutions with sterile BHI medium were performed in duplicate for each peptide in a sterile 96-well plate to a final volume of 50  $\mu\text{L}$  in each well. An aliquot (50  $\mu\text{L}$ ) of the cell suspension in BHI medium was added to each well, and the plate was incubated at 37 °C for 6 h. The absorbance at 590 nm was monitored. The MIC was defined as the concentration of peptide required for complete inhibition of growth (no change in the absorbance at 590 nm).

**Minimal Bactericidal Concentration Determination.** The MIC assay was performed as described above. After incubation for 6 h at 37 °C and determination of the MIC, selected wells with complete inhibition of growth were diluted 100-fold with sterile BHI medium. Plating was performed by spreading 100  $\mu\text{L}$  of each of these solutions on a solidified mixture of 2% bacteriological agar in BHI medium and incubating at 37 °C overnight. After incubation, the number of colonies on each plate was counted and compared with a control plate containing approximately  $10^3$  colony forming units of the same strain of bacteria without peptide.

**Hemolysis Assay.** Human erythrocytes (hRBC) were collected and stored refrigerated in a Becton Dickinson vacu-taner containing the anticoagulant EDTA for  $\leq 1$  day. The hRBC were collected by centrifugation and washed with TRIS-buffered saline (10 mM TRIS, 150 mM NaCl, pH 7.2) three times or until the supernatant was clear. The cells were then diluted with TRIS-buffered saline to a final concentration of 0.25% (v/v) and stored on ice for  $\leq 1$  h. Two-fold serial dilutions with TRIS-buffered saline were performed in duplicate for each peptide in a 96-well plate to a final volume of 20  $\mu\text{L}$  in each well. An aliquot (80  $\mu\text{L}$ ) of the 0.25% hRBC suspension was added to each well. Wells containing 20  $\mu\text{L}$  TRIS-buffered saline with 80  $\mu\text{L}$  hRBC suspension served as a negative control. The plate was incubated at 37 °C for 1 h and then centrifuged for 5 min at 3500 rpm. An aliquot (50  $\mu\text{L}$ ) of the supernatant from each well was transferred to a new well of a 96-well plate containing 50  $\mu\text{L}$  water, and the OD at 415 nm was measured. Percent hemolysis was calculated as  $[(\text{OD}_{415} \text{ peptide} - \text{OD}_{415} \text{ buffer}) / (\text{OD}_{415} \text{ complete hemolysis} - \text{OD}_{415} \text{ buffer})] \times 100$ , where complete hemolysis was defined as the average hemolysis of all wells containing a final concentration of melittin ranging from 50 to 400  $\mu\text{g/mL}$ .

**Peptide-Induced  $\beta$ -Galactosidase Leakage from *B. subtilis*.** *B. subtilis* BAU102<sup>60</sup> was grown in trypticase soy broth with 10  $\mu\text{g/mL}$  erythromycin and 34  $\mu\text{g/mL}$  chloramphenicol to ensure retention of *vanRS* and of *lacZ*, respectively. The cells were grown at 37 °C to an absorbance of 0.6 at 660 nm. Growth of the bacteria to the same absorbance each time was required to ensure reproducibility. The cells were collected by centrifugation and resuspended in fresh medium to remove residual  $\beta$ -galactosidase ( $\beta$ -gal). Aliquots (10  $\mu\text{L}$ ) of peptide stock solutions (200  $\mu\text{g/mL}$ ) were added to wells in a sterile 96-well plate. Bacterial suspension (90  $\mu\text{L}$ ) was then added to the wells to give a total volume of 100  $\mu\text{L}$  (final peptide concentration: 20  $\mu\text{g/mL}$ ). The final peptide concentration used in this assay was above the MIC in all cases. The plates were incubated at room temperature for 1 h to allow for the release of  $\beta$ -gal. After the incubation period, the plate was centrifuged for 5 min at 5000 rpm to remove all cells and cellular debris. An aliquot (80  $\mu\text{L}$ ) of the supernatant was removed and placed in a separate well. The enzymatically cleavable molecule 4-methyl-umbelliferyl  $\beta$ -galactoside (MUG) was used as a fluorescent indicator of  $\beta$ -gal. An aliquot of MUG in DMSO (20  $\mu\text{L}$ , 0.4 mg/mL) was added to the well, and fluorescence was monitored over time. Initial velocities of the enzymatic reaction were obtained from the linear plot of fluorescence versus time. Water without peptide was used as a negative control.

**RP-HPLC Assay.** Each  $\beta$ -peptide solution (50  $\mu\text{L}$ , 0.33 mg/mL  $\beta$ -peptide in a solution of 0.038% TFA in water) was injected onto a Vydac C4 analytical column (0.46  $\times$  25 cm, 5  $\mu$  particles). A linear gradient of 25–50% solvent B over 50 min or 20–50% B over 60 min was employed.

**Acknowledgment.** This work was supported by the NIH (GM56414). T.L.R. was supported in part by an NSF predoctoral fellowship, and E.A.P. was supported in part by an NIH Biotechnology training grant. CD data were obtained at the NSF-supported Biophysics Instrumentation Facility at UW-Madison. We thank Prof. Daniel H. Rich for advice on peptide synthesis, Dr. Gary Case for special assistance with the peptide synthesizer, and Prof. David Andes for advice on MBC determinations.

JA0270423

(79) Creighton, T. E. *Proteins: Structures and Molecular Principles*, 2nd ed.; W. H. Freeman and Company: New York, 1993; p 14.